Indian Journal of Radio & Space Physics
Vol. 35, December 2006, pp. 435-442

# Analysis of notch-loaded patch for dual-band operation

Shivnarayan & Babau R Vishvakarma*

Department of Electronics Engineering, Institute of Technology, Banaras Hindu University, Varanasi 221 005, India

E-mail: * brvish@bhu.ac.in

*Received 27 May 2005; revised 4 May 2006; accepted June 2006*

Analysis of notch loaded rectangular patch antenna for dual-band operation has been proposed, in which dual frequency behaviour is obtained by notch loading. The theoretical analysis is based on modal expansion cavity model. The resonance frequency changes with the variation in the length and width of the notch. Thus the input impedance, VSWR, return loss and bandwidth are calculated. The obtained resonance frequency ratio is variable from 1.17 to 1.77 with the length and width of the notch.

**Keywords:** Notched patch antenna, Dual-band patch antenna, Rectangular patch

**PACS NO.:** 84.40. Ba

**IPC Code:** H01Q9/00; H01Q21/00; H01Q23/00

## 1 Introduction

Microstrip antennas are popular for their attractive features such as low profile, light weight, low cost, ease of fabrication and integration with RF devices[1-2]. In the recent years, radar and communication system, such as global positioning system (GPS), synthetic aperture radar (SAR), often require dual frequency patch antennas to avoid the use of two different antennas. An ideal dual frequency antenna should have a similar performance in both operating modes, in terms of radiation properties and matching. In general, three techniques have been mentioned in the literature[3] to obtain dual frequency behaviour. These are identified as:

(i) Orthogonal mode of polarization

(ii) Multi-resonator antennas and

(iii) Reactively loaded antennas

Among these, the reactive loaded antennas are one of the most popular techniques to obtain the dual frequency behaviour. In this case, dual resonance is obtained by introducing the slots parallel to radiating edges of the patch[4], co-axial[5] or microstrip stubs[6] at the radiating edges of the patch. This does not allow a frequency ratio higher than 1.2. The higher frequency ratio can be obtained by using two lumped capacitors connected from patch to the ground plane[7]. The frequency ratio from 1.3 to 3 has also been obtained by the simultaneous use of slots and short circuit[8]. Another kind of reactive loading can be introduced to get higher ratio by cutting a notch in the patch parallel to the current lines. The notch loading allows one to obtain two resonant frequencies due to strong interaction between the main patch and the notch resonant frequency[9]. Notch loading is also a good solution to minimize and enhance the impedance mismatch and bandwidth[10], respectively. Almost similar radiation patterns for the rectangular and notch-loaded patch antennas confirm that the current distributions are not much affected by the notch cut in the patch[9].

In the present paper the analysis of notch-loaded rectangular microstrip patch antenna has been carried out using the concept of equivalent circuit theory. In the present work the study of effect of notch length and width on the resonance frequencies has been investigated. It is found that the frequency ratio of two resonances can be varied from 1.18 to 1.77 with the notch dimensions.

## 2 Theoretical considerations

The proposed antenna geometry is shown in Fig. 1. The patch is fed by a co-axial probe.

The feed position is calculated by using modal expansion cavity model theory[11], for a 50 Ω co-axial cable. The notch has been cut along the patch width in such a way that it lies at a symmetrical distance from both length edges of the patch. According to the cavity model theory[12], a normal microstrip patch

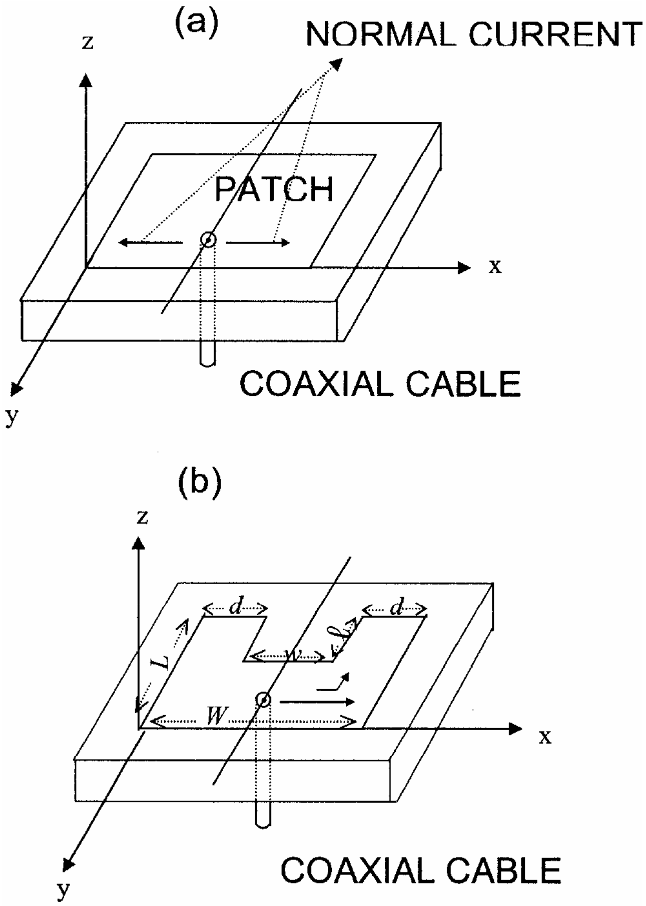

Fig. 1 — Geometry of (a) rectangular and (b) notched microstrip patch antenna

antenna can be modeled as parallel *RLC* circuit. The current flows from the feeding point to the top and bottom edges of the patch. Values of *L* and *C* are determined by the currents path length. When a notch is incorporated into the patch, the resonance feature changes. In this case, two current's flow in the patch[13]; one is the normal current which flows into the patch as shown in Fig. 1(a). It represents the initial *RLC* resonant circuit and resonates at the designed frequency of the patch as shown in Fig. 2(a). However, the other current flows around the notch as shown in Fig. 1(b) and hence the length of the current path increases. In this case, both electric and magnetic field discontinuities occur across the notch. So the effect of the notch will be both capacitive and inductive. These effects are modeled[14] as additional series inductance $\Delta L$ and series[15-16] capacitance $\Delta C$ to the initial resonant circuit as shown in Fig. 2(b). Therefore, the proposed antenna behaves as a dual resonant circuit.

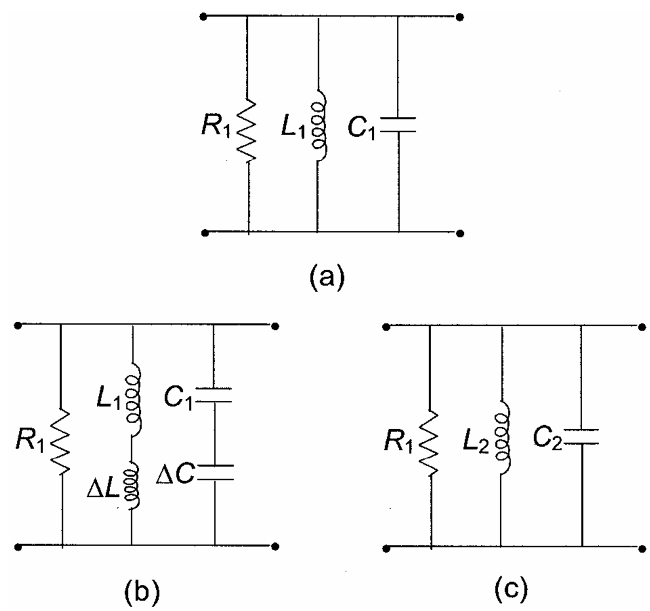

Fig. 2 — Equivalent circuit of (a) rectangular microstrip patch antenna, (b) that corresponding to the current flowing around the notch, i.e. due to notch effect on the patch and (c) simplified circuit of (b)

**2.1 Equivalent circuit**

The equivalent circuit corresponding to this current flowing on the patch is shown in Fig. 2(a), where $C_1$, $L_1$ and $R_1$ are the capacitance, inductance and radiation resistance of the patch, respectively and are given by[12]

$$C_1 = \frac{\varepsilon_e \varepsilon_0 LW}{2h} \cos^{-2}\left(\frac{\pi y_0}{L}\right) \qquad \ldots(1)$$

where $L$ = length of the patch

$W$ = width of the patch

$h$ = thickness of the substrate

$\varepsilon_e$ = effective dielectric constant

$$= \frac{\varepsilon_r + 1}{2} + \frac{\varepsilon_r - 1}{2}\left(1 + \frac{12}{W}\right)^{-\frac{1}{2}}$$

$\varepsilon_r$ = relative dielectric constant of the substrate

$y_o$ = feed point location along the *y*-axis, i.e., along the length of the patch

Also $$_1 = \frac{1}{{}_1.\omega_r^2} \qquad \ldots(2)$$

and $$R_1 = \frac{Q}{\omega\ C_1} \quad \ldots(3)$$

where $Q$ and $\omega_r$ are the quality factor and resonance frequency of the patch, respectively. The quality factor $Q$ is given by[12]

$$Q_r = \frac{c\sqrt{\varepsilon_e}}{4 f_r h}$$

where $c$ = velocity of light in free space and $f_r$ = resonance frequency of the patch.

The input impedance of the resonant circuit shown in Fig. 2(a) is calculated by

$$Z_{patch} = \frac{1}{\left(\frac{1}{R_1} + j\omega C_1 + \frac{1}{j\omega L_1}\right)} \quad \ldots(4)$$

The other current is flowing around the notch on the patch. The equivalent circuit corresponding to this current is shown in Fig. 2(b), where $C_1$, $L_1$, and $R_1$ have their usual meaning. Additional series inductance $\Delta L$ and capacitance $\Delta C$ due to notch effect are calculated[14,15], respectively as

$$\Delta L = \frac{h\mu_0 \pi}{8}(\lambda / L)^2 \quad \ldots(5)$$

where $\mu_0 = 4\pi 10^{-7}$ and $\lambda$ = equivalent length of the notch and

$$\Delta C = \left(\frac{\lambda}{L}\right).C_s \quad \ldots(6)$$

The term $C_s$ = gap capacitance and is given by Meshram and Vishvakarma[16].

The input impedance of the resonant circuit shown in Fig. 2(b) can be computed from the simplified circuit shown in Fig. 2(c) as

$$Z_{patch} = \frac{1}{\left(\frac{1}{R_1} + j\omega C_2 + \frac{1}{j\omega L_2}\right)} \quad \ldots(7)$$

where $$C_2 = \frac{C_1.\Delta C}{(C_1 + \Delta C)}$$

$$L_2 = L_1 + \Delta L$$

As already mentioned these two resonant circuits are coupled together and form a dual resonant circuit for dual band operation as shown in Fig. 3. Here both the inductive and capacitive coupling has been considered.

The coupling coefficient between these two resonators is given by[17]

$$C_p = \frac{1}{\sqrt{Q_1.Q_2}} \quad \ldots(8)$$

where $Q_1$ = quality factor of the resonant circuit due to normal current $= \frac{\omega L_1}{R_1}$

and $Q_2$ = quality factor of the resonant circuit due to notch effect $= \frac{\omega L_2}{R_1}$

The mutual inductance ($L_m$) and mutual capacitance ($C_m$) between two resonant circuits are given by[17]

$$L_m = \frac{C_p^2\left(L_1 + L_2\right) + \sqrt{C_p^2\left(L_1 + L_2\right)^2 + 4C_p^2\left(1 - C_p^2\right)L_1 L_2}}{2\left(1 - C_p^2\right)} \quad \ldots(9)$$

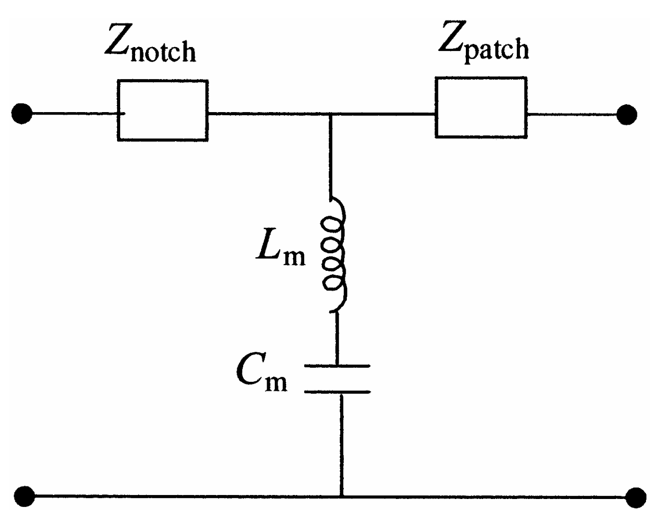


Fig. 3 — Equivalent circuit of notched rectangular patch antenna

$$C_m = \frac{-\left(C_1+C_2\right)+\sqrt{\left(C_1+C_2\right)^2-4C_1C_2\left(1-C_p^{-2}\right)}}{2} \quad \ldots(10)$$

Now the input impedance of the notched rectangular microstrip patch antenna can be computed from the simplified circuit shown in Fig. 3, as

$$Z_{in} = Z_{notch} + \left(\frac{Z_{patch}\,Z_m}{Z_{patch}+Z_m}\right) \quad \ldots(11)$$

where

$$Z_m = j\omega L_m + \frac{1}{j\omega C_m}$$

Using Eq. (11), the reflection coefficient, VSWR, return loss and bandwidth can be computed by[18]

$$\text{Reflection coefficient} = \Gamma = \frac{Z_0 - Z_{in}}{Z_0 + Z_{in}} \quad \ldots(12)$$

where $Z_0$ = characteristic impedance of the co-axial feed (50 Ω)

$$\text{VSWR} = S = \frac{1+|\Gamma|}{1-|\Gamma|} \quad \ldots(13)$$

$$\text{Bandwidth} = \frac{S-1}{Q\sqrt{S}} \quad \ldots(14)$$

$$\text{and Return loss} = 20\log|\Gamma| \quad \ldots(15)$$

## 3 Designed parameters

For designing the notched rectangular microstrip patch antenna, following parameters were used

| | |
|---|---|
| Design frequency | = 3.0 GHz |
| Free space wavelength (λ) | = 100 mm |
| Dielectric constant (R-T Duroid) | = 2.2 |
| Loss tangent | = $\tan\delta$ = 0.0013 |
| The thickness of the substrate (*h*) | = 0.016 λ |
| Length of the patch (*L*) | = 0.329 λ |
| Width of the patch (*W*) | = 0.395 λ |
| Location of feed point (*x*, *y*) | = (19.75, 9.85) mm |

## 4 Calculations

The input impedance of the notch loaded patch is calculated using Eq. (11) for different notch length and width. The data thus obtained are shown in Figs 4 and 5. The variation of lower and upper resonance frequencies with notch length and width are shown in Figs 6[(a)-(c)], and 7[(a)-(c)], respectively. The variation of difference of upper and lower resonance frequencies with notch length and width are shown in Figs 8(a) and 8(b), respectively. The value of VSWR and return loss are calculated using Eqs (13) and (15), for different values of notch length and width. The resulting data are presented in Figs 9-10 and Figs 11-12. The bandwidth is calculated using Eq. (14) for different notch length and width. The resulting data are presented in Tables 1 and 2.

## 5 Discussion of result

The variation of input impedance with frequency for different notch length for a given notch width are shown in Fig. 4. It is observed that the notch loaded antenna shows dual resonance, in which lower resonance frequency increases with increasing notch length, whereas upper resonance frequency decreases with notch length. This indicates that difference between two resonances is large at small notch length and it decreases with increasing notch length. This is also indicated by Fig. 6[(a)-(c)].

The variation of input impedance with frequency for different notch widths for a given notch length are shown in Fig. 5. It is observed that lower and upper resonance frequencies remain almost constant with the notch width up to 0.08λ for a given notch length; thereafter it decreases. This is also observed from Fig. 7[(a)-(c)].

It is further noted that the ratio of upper to lower resonance frequency ($f_2/f_1$) decreases with increasing notch length for all the notch width as shown in Table 3. In this case the frequency ratio varies from 1.17 to 1.77, with the notch length from 0.02 λ to 0.14 λ, whereas the ratio remains almost constant with the notch width for all notch length as shown in Table 4. From Fig. 8(a) it is observed that the difference between two resonances decreases with notch length for a given notch width. Whereas this difference remains almost constant with the notch width up to 0.08 λ for a given notch length, thereafter it decreases as shown in Fig. 8 (b).

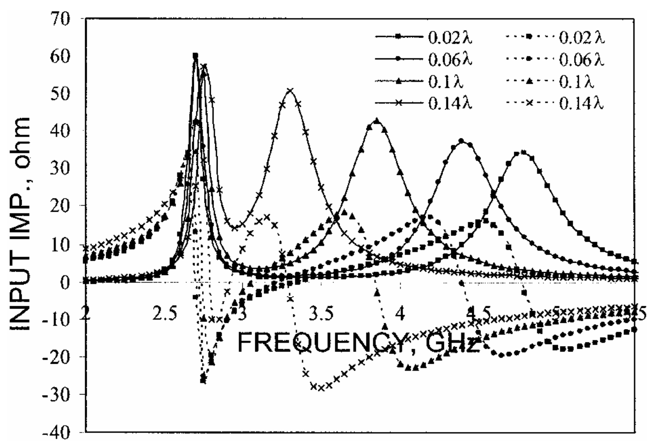


Fig. 4 — Variation of input impedance with frequency for different notch length for a given notch width

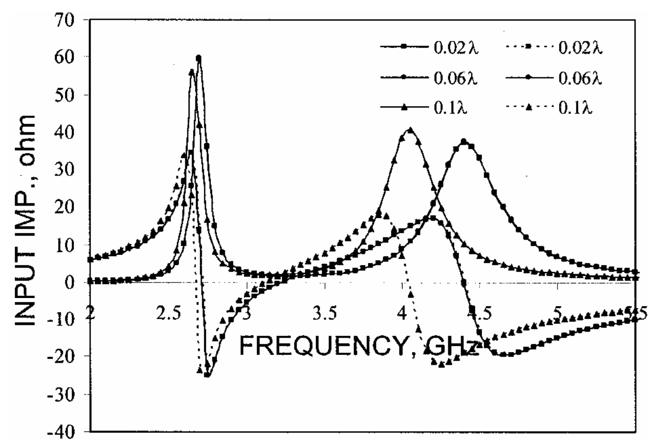


Fig. 5 — Variation of input impedance with frequency for different notch width for a given notch length

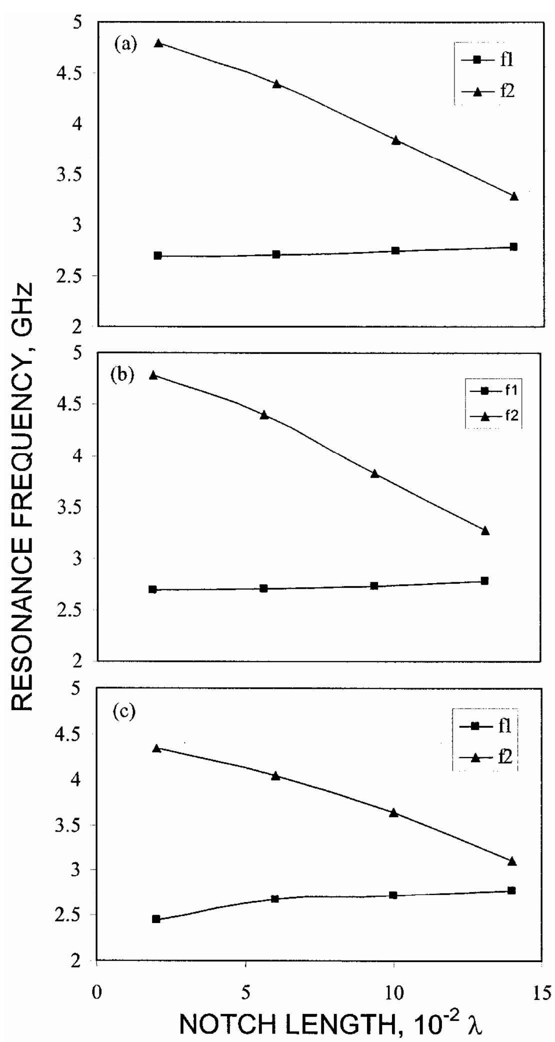


Fig. 6 — Variation of lower and upper resonance frequencies with notch length for a given notch width (a) 0.02 λ, (b) 0.06 λ, and (c) 0.10 λ

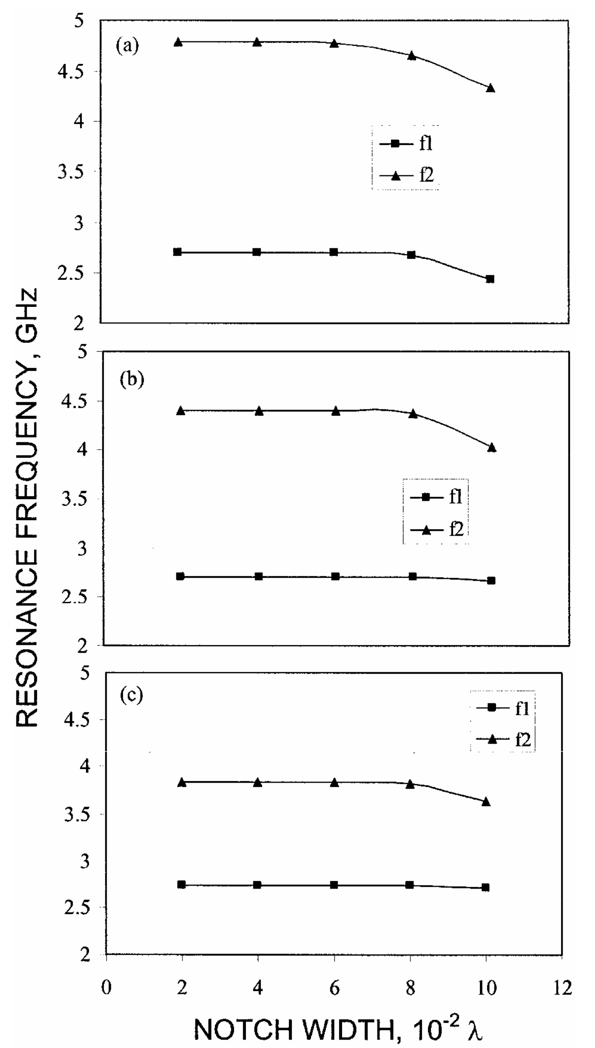


Fig. 7 — Variation of lower and upper resonance frequencies with notch width for a given notch length (a) 0.02 λ, (b) 0.06λ, and (c) 0.10 λ

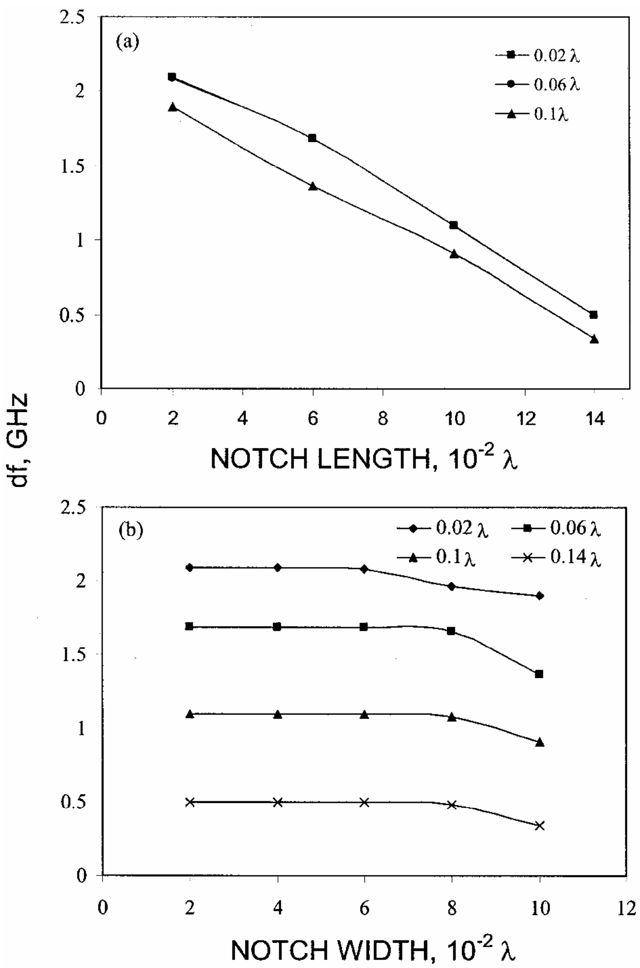


Fig. 8 — Variation of difference of upper and lower resonance frequency with (a) notch length for a given notch width and (b) notch width for a given notch length

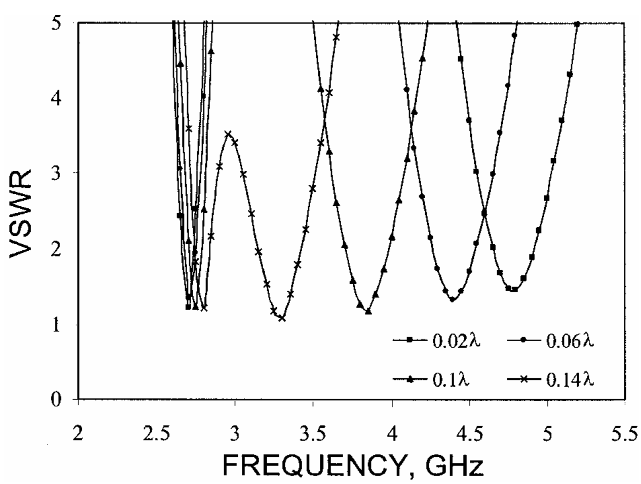


Fig. 9 — Variation of VSWR with frequency for different notch length for a given notch width = 0.06 λ

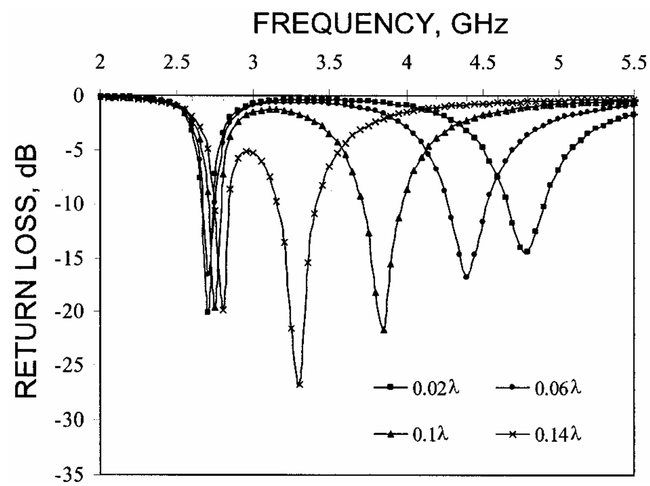


Fig. 10 — Variation of return loss with frequency for different notch length for a given notch width = 0.06 λ

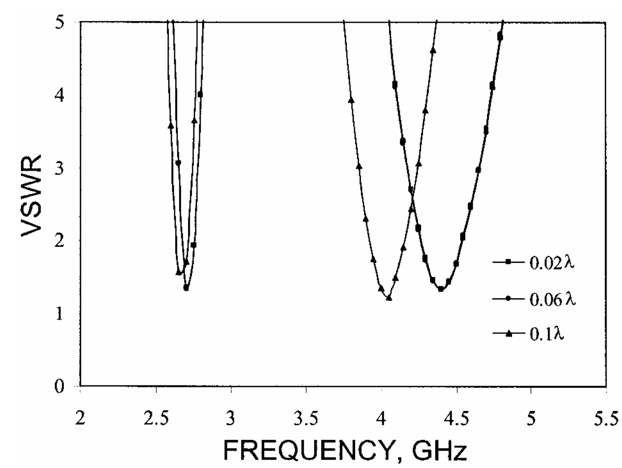


Fig. 11 — Variation of VSWR with frequency for different notch width for a given notch length = 0.06 λ

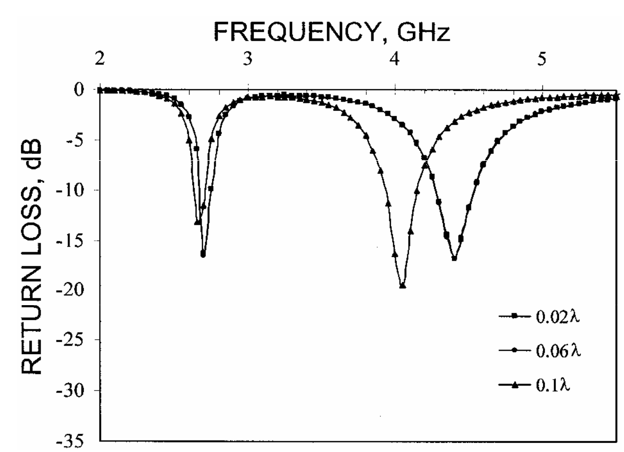


Fig. 12 — Variation of return loss with frequency for different notch width for a given notch length = 0.06 λ

Table 1 — Variation of % Bandwidth with notch length for a given notch width

| Notch length, mm | Notch width, mm | | | | | |
|---|---|---|---|---|---|---|
| | 2.0 | | 6.0 | | 10.0 | |
| | Band 1 | Band 2 | Band 1 | Band 2 | Band 1 | Band 2 |
| 2 | 2.74 | 5.65 | 2.78 | 5.57 | 2.70 | 4.67 |
| 6 | 2.84 | 6.29 | 2.80 | 6.27 | 2.73 | 5.77 |
| 10 | 2.95 | 7.55 | 2.95 | 7.24 | 2.94 | 6.77 |
| 14 | 3.52 | 8.55 | 3.52 | 8.46 | 4.29 | 8.59 |

Table 2 — Variation of % bandwidth with notch width for a given notch length

| Notch width, mm | Notch length, mm | | | | | | | |
|---|---|---|---|---|---|---|---|---|
| | 2.0 | | 6.0 | | 10.0 | | 14.0 | |
| | Band 1 | Band 2 | Band 1 | Band 2 | Band 1 | Band 2 | Band 1 | Band 2 |
| 2 | 2.78 | 5.09 | 2.99 | 6.24 | 2.95 | 7.22 | 3.51 | 8.43 |
| 6 | 2.78 | 5.07 | 2.99 | 6.24 | 2.95 | 7.22 | 3.51 | 8.43 |
| 10 | 2.58 | 5.68 | 2.76 | 6.75 | 2.87 | 7.77 | 3.35 | 8.96 |

Table 3 — Variation of frequency ratio ($f_2/f_1$) with notch length for a given notch width

| Notch length (mm) | Notch width, mm | | |
|---|---|---|---|
| | 2.0 | 6.0 | 10 |
| 2 | 1.77576 | 1.771598 | 1.733135 |
| 6 | 1.622419 | 1.621313 | 1.61226 |
| 10 | 1.400219 | 1.399489 | 1.393939 |
| 14 | 1.179598 | 1.179662 | 1.174335 |

Table 4 — Variation of frequency ratio ($f_2/f_1$) with notch width for a given notch length

| Notch width, mm | Notch length, mm | | | |
|---|---|---|---|---|
| | 2.0 | 6.0 | 10.0 | 14.0 |
| 2 | 1.77576 | 1.622419 | 1.400219 | 1.179598 |
| 6 | 1.775389 | 1.622419 | 1.400219 | 1.179598 |
| 10 | 1.771598 | 1.621313 | 1.399489 | 1.179662 |

The variation of VSWR with frequency for different notch length for a given notch width are shown in Fig. 9. It is observed that the value of VSWR remains almost constant (1.23) with notch length corresponding to lower resonance frequency, whereas it decreases from 1.46 to 1.10 with notch length corresponding to upper resonance frequency. This indicates that matching condition improves with the increase in notch length corresponding to upper resonance frequency. Therefore the bandwidth of upper resonance frequency is greater than that of lower resonance frequency as shown in Table 1. This is also corroborated from return loss data shown in Fig. 10 for different notch length for a given notch width.

The variation of VSWR with frequency for different notch width for a given notch length are shown in Fig. 11. It is observed that the value of VSWR remains almost constant with the notch width up to 0.06 λ for a given notch length corresponding to both lower and upper resonance frequency. Thereafter it increases (from 1.23 to 1.55) for lower resonance frequency, while it decreases (from 1.34 to 1.24) for upper resonance frequency. This indicates that matching condition decreases for lower resonance frequency, whereas it increases for upper resonance frequency after 0.06 λ notch width. Therefore bandwidth remains almost constant up to 0.06 λ notch width for a given notch length corresponding to both lower and upper resonance frequency; thereafter it decreases for band-1 while it increases for band-2 as shown in Table 2. This is also corroborated from return loss data shown in Fig. 12 for different notch width for a given notch length. The optimum design for maximum bandwidth is found to be; length of the notch = 0.14 λ and width = 0.10 λ. This is also obvious from Table 1. Similar observations were also made by Palit and Hamadi[9].

## 6 Conclusions

It is observed that the properly designed notched patch antenna exhibited dual frequency operation. The resonance frequency ratio can be varied from 1.17 to 1.77 with the notch dimension. The bandwidth can also be changed from 2.70% to 4.29% for band 1 and from 4.67% to 8.59% for band 2, with the notch length for a given notch width. Therefore the proposed antenna can be used for mobile communications.

## Acknowledgement

One of the authors (Shivnarayan) is very grateful to University Grants Commission, New Delhi for providing financial assistance through junior research fellowship.

## References


1 James J R & Hall P S, *Handbook of Microstrip Antennas* (Peter Peregrinus, UK), 1989.

2 Gao S C & Zhong S S, Dual polarized microstrip antenna array with high isolation fed by co-planar network, *Microw Opt Tech Lett (UK),* 19 (1998) 214.

3 Maci S, Biffi G & Gentili, Dual frequency patch antennas, *IEEE Trans Antennas Propag (USA),* 39 (1997) 13.

4 Maci S, Biffi G Gentili, Piazzesi P & Salvador C, Dual-band slot loaded patch antenna, *IEE Proc H Microw Antennas Propag (USA),* 142 (1995) 225.

5 Richards W R, Davidson S E & Long S A, Dual-band reactively loaded microstrip antenna, *IEEE Trans Antennas Propag (USA),* 33 (1985) 556.

6 Davidson S E, Long S A & Richards W R, Dual-band microstrip antenna with monolithic reactive loading, *Electron Lett (UK),* 21 (1985) 936.

7 Waterhouse R B & Shuley N V, Dual frequency microstrip rectangular patches, *Electron Lett (UK),* 28 (1992) 606.

8 Wong B F & Lo Y T, Microstrip antenna for dual frequency operations, *IEEE Trans Antennas Propag (USA),* 32 (1984) 938.

9 Palit S K & Hamadi A, Design and development of wide-band and dual-band microstrip antennas, *IEE Proc H Microw Antennas Propag (UK)*, 146 (1999) 35.

10 Robert B, Rozban T & Papiernik A, Compact patch antenna integrates monolithic amp, *Microwave RF (USA)*, 34 (1995) 115.

11 Ballanis C A, *Antenna Theory Analysis and Design* (Harper & Row): New York, 1938.

12 Bahl I J & Bhartia P, *Microstrip Antennas* (Artech House): Massachusetts, 1980, 48 -57.

13 Yang F, Zhang X X, Ye X & Rahamat-Samii Y, Wide-band E-shaped patch antennas for wireless communications, *IEEE Trans Antennas Propag (USA)*, 49 (2001) 1094.

14 Zhang X X & Yang Fan, Study of slit cut on a microstrip antenna and its applications, *Microw Opt Tech Lett (USA)*, 18 (1998) 297.

15 Wolfgang & Hoefer J R, Equivalent series inductivity of a narrow transverse slit in microstrip, *IEEE Trans on Microw Theory Tech (USA)*, 25 (1997) 822.

16 Meshram M K & Vishvakarma B R., Gap-coupled microstrip array antenna for wide-band operation, *Int J Electron (UK)*, 88 (2001) 1161.

17 Pandey V K & Vishvakarma B R, Theoretical analysis of linear array antenna of stacked patches, *Indian J Radio & Space Phys*, 34 (2005) 125.

18 Derneryed A G & Lind A G, Extended analysis of rectangular microstrip antennas, *IEEE Trans Antennas Propag (USA)*, 27 (1979) 846.